ORIGINAL ARTICLE

Cytometry
PART A
Journal of the International Society for Advancement of Cytometry

Upgrading Time Domain FLIM Using an Adaptive Monte Carlo Data Inflation Algorithm

Dave Trinel,[1] Aymeric Leray,[1] Corentin Spriet,[1] Yves Usson,[2] Laurent Héliot[1]*

[1]Interdisciplinary Research Institute, University of Lille - Nord de France, USR 3078 CNRS, Biophotonique Cellulaire Fonctionnelle, Parc de la Haute Borne, Villeneuve d'Ascq 59658, France

[2]Laboratoire TIMC-IMAG, Joseph Fourier University, UMR 5525 CNRS, RFMQ, Domaine de la Merci, La Tronche 38710, France

Received 18 December 2010; Revision Received 17 February 2011; Accepted 1 March 2011

Dave Trinel and Aymeric Leray contributed equally to this work.

Grant sponsors: CNRS (GdR2588 and MRCT), Région Nord Pas de Calais, European Regional Developmental Funds, Leica Microsystems partnership, Agence Nationale de la Recherche; Grant number: ANR 07-PFTV-01101.

*Correspondence to: Laurent Heliot, Interdisciplinary Research Institute, Parc de la haute borne, 50 avenue de Halley, BP 70478, 59658 Villeneuve d'Ascq, Cedex

Email: laurent.heliot@iri.univ-lille1.fr

Published online 12 May 2011 in Wiley Online Library (wileyonlinelibrary.com)

DOI: 10.1002/cyto.a.21054

Abstract

Fluorescence Lifetime Imaging Microscopy (FLIM) is a powerful technique to investigate the local environment of fluorophores in living cells. To correctly estimate all lifetime parameters, time domain FLIM imaging requires a high number of photons and consequently long laser exposure times. This is an issue because long exposure times are incompatible with the observation of dynamic molecular events and induce cellular stress. To minimize exposure time, we have developed an original approach that statistically inflates the number of collected photons. Our approach, called Adaptive Monte Carlo Data Inflation (AMDI), combines the well-known bootstrap technique with an adaptive Parzen kernel. We here demonstrate using both Monte Carlo simulations and live cells that our robust method accurately estimate fluorescence lifetimes with exposure time reduced up to 50 times for monoexponential decays (corresponding to a minimum of 20 photons/pixel), and 10 times for biexponential decays (corresponding to a minimum of 5,000 photons/pixel), compared to standard fitting method. Thanks to AMDI, in Förster resonance energy transfer experiments, it is possible to estimate all fitting parameters accurately without constraining any parameters. By reducing the commonly used spatial binning factor, our technique also improves the spatial resolution of FLIM images. © 2011 International Society for Advancement of Cytometry

Key terms

Time Correlated Single Photon Counting (TCSPC); Förster Resonance Energy Transfer (FRET); Least Square Method (LSM) curve fitting; Monte Carlo; Parzen kernel; bootstrap; Fluorescence Lifetime Imaging Microscopy (FLIM); molecular interactions; live cell

THE characterization of dynamic interactions between biomolecules in living cells or tissues is a major field of biological and medical research. Fluorescence microscopy is well-adapted for studying these molecular interactions and their organization in cells, tissues, and small organisms (1,2). Thanks to fluorescent probes, it has become possible to track molecules and quantify their dynamics. However, fluorophores properties may be affected by a number of environmental factors such as the composition, interactions, and dynamics of molecular species, and therefore bias interpretations based on fluorescence intensity. To avoid this problem, different microscopy techniques measuring various photon properties such as the fluorescence lifetime (3,4) must be used in combination.

Fluorescence Lifetime Imaging Microscopy (FLIM) is particularly adapted to visualizing and measuring Förster Resonance Energy Transfer (FRET) occurring between interacting proteins in tissues or cells (5,6). To measure fluorescence lifetime, many methods exist, which may be divided into two main groups: frequency domain (7,8) and time domain methods (9–11). In this article, we limited our study to the second group.

In time domain methods, fluorescent samples are repeatedly excited by short pulses of light, and the time delays between these pulses and the emitted fluorescence photons are recorded as fluorescence decay histograms $I(t)$. Technically, this can be

done by using a Time Correlated Single Photon Counting (TCSPC) system (10), or by measuring the fluorescence signal either using a time-gated detector (12), or a streak camera (13). Regardless of the technique applied, the theoretical fluorescence intensity profile $I(t)$ is defined as:

$$I(t) = \sum_i a_i \exp\left(-\frac{t}{\tau_i}\right) \text{ with : } \sum_i a_i = 1 \qquad (1)$$

Where a_i is the contribution and τ_i is the lifetime of the species *i*. In most cases, these values can be experimentally determined by successively minimizing the difference between collected data and theoretical values (fitting method). When several fluorescent species are present in the sample (such as in FRET experiments), the precise estimation of all fitting parameters requires large numbers of both photons and temporal channels (14). In this study, we measured fluorescence lifetime using the TCSPC technique with 256 temporal channels. As previously mentioned, the robustness of the curve fitting method is also strongly dependent on the statistics of the collected data. Large numbers of photons are indeed necessary to precisely estimate all fitting parameters. The number of counted photons may be increased either by increasing laser power or by extending acquisition time. However both options are harmful: a higher laser power causes photo-damage in live cells (15), and a longer acquisition time requires a longer laser excitation time thus inducing cellular stress (16) and precludes the observation of rapid molecular events.

In a previous study, we optimized acquisition conditions and demonstrated that the acquisition of a 128 × 128 pixels FLIM image with an average of 10^3 photons per pixel required 300 s to avoid photobleaching, phototoxicity, and photodamage (11).

Unfortunately, such long acquisition times are incompatible with the observation of most dynamics processes involved in the regulation of cells and organisms (17).

To address this issue, many recent efforts focused on reducing acquisition time by developing high-speed FLIM techniques, using specific detectors and dedicated electronic cards (18–20). In contrast, the work presented here uses a standard TCSPC FLIM acquisition system. We propose an original solution, based on a statistical data inflation method we called Adaptive Monte Carlo Data Inflation (AMDI), to decrease acquisition time and improve FLIM studies in live cells.

First, we performed Monte Carlo simulations of TCSPC histograms with monoexponential and biexponential decays of known parameters to demonstrate the robustness and efficiency of our approach. Second, we applied this approach to living samples and showed that accurate lifetime estimation is possible with exposure time reduced by up to 50 times for monoexponential decays (corresponding to a minimum of 20 photons/pixel), and 10 times for biexponential decays (corresponding to a minimum of 5,000 photons/pixel), compared to standard fitting method. The final section of the article discusses the benefits and limitations of the AMDI approach.

Materials and Methods

Two-Photon Fluorescence Lifetime Microscopy

Our TCSPC FLIM system was built on a commercial confocal microscope (Leica TCS SP5 X, Leica Microsystems). Fluorescent samples were excited at 900 nm using a Ti:Sa pulsed laser source (Chameleon Ultra2, Coherent). The two-photon excitation fluorescence was collected between 500 and 530 nm (with a band pass filter XF3080, Omega Optical), using a high temporal resolution detector (MCP-PMT model R3809U-52, Hamamatsu) (11). The temporal fluorescence histograms were reconstructed with a dedicated photon-counting and timing electronic card (SPC 830, Becker & Hickl). All measured FLIM histograms were acquired using the TCSPC technique with 256 channels separated by a temporal resolution of 0.0488 ns, resulting in a total time window of 12.5 ns.

Monte Carlo Simulation of FLIM Data Sets

To compare the curve fitting estimation with or without AMDI, a large number of data sets or photon histograms with controlled and known parameters were generated with a Monte Carlo approach on a standard computer (21). The algorithm used to compute the simulated fluorescence decay histograms was previously described by Spriet et al. (22). The simulated FLIM histograms were built with the same parameters as those previously described (total time window of 12.5 ns divided between 256 temporal channels). For each condition, we generated 16,384 simulated decays, which is a sample size large enough to give good agreement with a Gaussian sampling distribution.

Curve Fitting Method

The theoretical fluorescence intensity profile $I(t)$ reported in Eq. (1) does not accurately describe the measured intensity decays. In real FLIM experiments, we also need to take into account both the Instrumental Response Function (IRF) of the acquisition system, and the background level noted *b*. The detected intensity profile $F(t)$ is then equal to the convolution product of the IRF, and the theoretical intensity profile with an added background *b*, which can be described as (23):

$$F(t) = \text{IRF} \otimes (b + I(t)) = \text{IRF} \otimes \left(b + \sum_i a_i \exp\left(-\frac{t}{\tau_i}\right)\right) \qquad (2)$$

Where a_i is the fraction of species *i* and τ_i is the fluorescence lifetime of species *i*.

To evaluate fluorescence lifetime based on experimental intensity decays, we performed a least square nonlinear regression fitting method (24), which consists in minimizing the difference between experimental points and the theoretical intensity profile described by Eq. (2).

In this study, we used the common Levenberg-Marquardt algorithm to minimize the error function $\chi^{(2)}$ between experimental data points (d_i) and the theoretical values, obtained from the model (f_i). $\chi^{(2)}$ is defined as:

$$\chi^{(2)} = \frac{1}{N-p}\sum_{i=1}^{N}\frac{(d_i - f_i)^2}{d_i} \quad (3)$$

Where N is the number of data points and p is the number of fitting parameters.

For the analysis of FLIM images, we used the commercially available SPC Image software (version 3.1.0.0, Becker & Hickl GmbH), which also uses the Levenberg-Marquardt algorithm. We used the multiexponential decay fitting model for simulated decays, and the incomplete multiexponential decay fitting model for experimental FLIM images (with one or two components), as well as the following parameters: minimal parameter constraints (min lifetime: 20 ps; max lifetime: 30,000 ps; min ratio: 1), standard algorithmic settings (20 iterations and $\Delta\chi^2 = 0.001$) and trapezoid integration.

The Adaptive Monte Carlo Data Inflation Algorithm

Estimating the probability density function of a variable to extract potentially missing information from a small experimental sample is a common problem in statistics. The original AMDI approach we developed combines two techniques: the Parzen kernel and the bootstrap.

The Parzen kernel is a nonparametric estimation of the probability density function of a random variable. If $x_1, x_2, \ldots, x_N$ are independent and identically distributed random variables with a probability density function f, the kernel density approximation of f is defined as (25)

$$f_g(x) = \frac{1}{N \times g}\sum_{i=1}^{N} k\left(\frac{x - x_i}{g(x)}\right) \quad (4)$$

Where k is a kernel (which is a symmetric function whose integral is one) and g is a smoothing function. In this study, we used a standard Gaussian kernel, with a mean of 0 and a variance of 1. Note that the smoothing function g indirectly controls the variance of this Gaussian kernel as

$$k\left(\frac{x - x_i}{g(x)}\right) = \frac{1}{\sqrt{2\pi}}\exp\left(-\frac{(x - x_i)^2}{2g(x)^2}\right) \quad (5)$$

In this study, we used an adaptive smoothing factor over x, which is based on preexisting knowledge about the properties of the density function to be estimated. When the total number of photons N was low ($N < 5{,}000$ photons), we used the inverse function of the theoretical law of fluorescence photon emission, which corresponds to a smoothing factor $g(x) = \ln(x)$. For higher total photon numbers ($N > 5{,}000$ photons), there were no empty temporal channels, and it was not necessary to spread the information temporally as much as previously. We thus used a lower smoothing factor: $g(x) = \log(x)$. The width of the Parzen kernel increases with the temporal channel, to maintain a virtually constant signal-to-noise ratio for each temporal channel, and to compensate for the poor signal-to-noise ratio occuring with longer emission photon times, when photon numbers are lower.

The bootstrap technique (26,27) is a statistical inference method. This resampling method relies on the generation of a huge number of simulated data samples, based on a small experimental data set.

We combined both Parzen kernel and boostrap techniques to estimate the parameters of collected fluorescence decays, by generating artificial data samples that preserve the properties of the original samples, and guarantee a robust estimation of statistical parameters. The AMDI algorithm (Fig. 1) we developed to generate amplified fluorescence decay histogram from small data set is as follows:

The fluorescence decay histogram called $h(t)$ was built from H_m and H_s. H_m represents the measured set of photon arrival events e_i, where $H_m = \{e_1, e_2, \ldots, e_p\}$, and p is the number of events. H_s is the simulated sets where $H_s = \{s_1, s_2, \ldots, s_q\}$, and q is the number of simulated photon events which is at least an order of magnitude greater than p. We call $G(\mu, \sigma)$ a Gaussian random generator with mean μ and standard deviation σ. We assume that the photon shot noise for any photon event e_i follows a Poisson distribution, and therefore that σ is equal to $g.h(e_i)^{1/2}$, where g is the previously described smoothing function.

1. Set a loop counter c to 1 and initialize H_s with a size of q.
2. Generate a value i (comprised between 1 and p) from a random number generator with a uniform probability
3. Set x to e_i
4. Set s_c to $G(x, g.h(x)^{1/2})$
5. Add s_c to H_s
6. Increment c
7. While $c < q$ repeat steps 2 to 6
8. Build a new fluorescence decay histogram based on the new H_s set.

This algorithm is applied to all the photons which make-up the fluorescence intensity decays, but not to those present in the first temporal channels (background only). For these ones, the mean number of background photons per pixel is inflated using the same coefficient factor and spread over the first temporal channels without smoothing function ($g = 1$).

We implemented the AMDI algorithm into a home-made software named TITAN (IRI, USR 3078 CNRS, BCF).

The AMDI algorithm generates artificial data samples by inflating original samples with a coefficient factor. We tested different values to determine the optimal inflation factor needed to obtain reliable results with the fitting method. We demonstrated that fluorescence lifetime precision was unchanged when the number of photons per pixel was greater than 10,000 for monoexponential decays, and 100,000 for biexponential decays (data not shown). Therefore, to correctly estimate the density probability function in subsequent studies, we adjusted the inflation factor to obtain at least 10,000 photons per pixel for monoexponential decays and 100,000 for biexponential decays.

We emphasize that the AMDI algorithm conserves the initial photons emission law during inflation, and so prevents

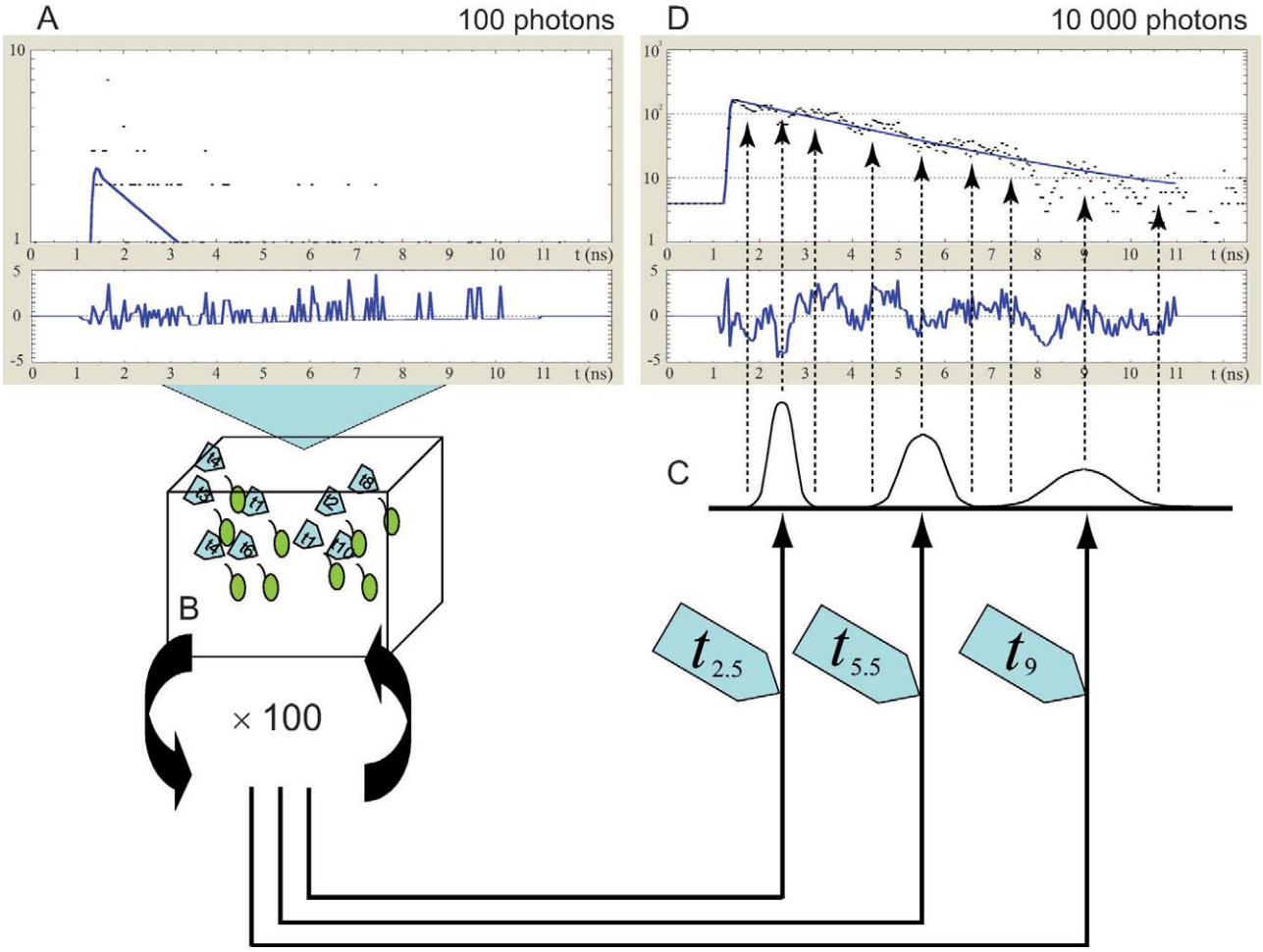

Figure 1. Scheme of the AMDI algorithm. From an initial fluorescence intensity decay constituted with few photons (**A**), each photon is allocated to its temporal channel number and put in a virtual urn (**B**). From this urn, an original photon with temporal channel number t_x is randomly drawn and duplicated to a virtual photon with the same time t_x (bootstrap technique). The original photon is then moved back to the urn. The virtual photon is allocated to a new channel number with an adaptive Parzen kernel, and added to the original decay (**C**). The process is repeated until the AMDI factor is reached (100 in this case). Finally, the total photon number is inflated by this factor (**D**). [Color figure can be viewed in the online issue which is available at wileyonlinelibrary.com]

the artifacts, which may be caused by using a statistical inference method with an adaptive Parzen kernel width along the temporal channel. In addition, it is important to notice that the AMDI algorithm should not degrade the IRF of the experimental system for estimating accurately all fitting parameters. The IRF was then included in the adaptive Parzen kernel width calculation, and we checked that it was unaffected by the AMDI algorithm (data not shown).

Plasmids, Cell Culture, Transfection, and FLIM Measurements

U2OS and HEK293 cells were grown in Dulbecco's modified Eagle's medium (Invitrogen), supplemented with 10% fetal calf serum and 1% penicillin-streptomycin (Invitrogen), and were seeded 12 h before transfection in 6-well dishes containing 32 mm diameter glass coverslips. Transient transfections were performed according to manufacturer's recommendations, using FugeneHD (Roche Diagnostic) for plasmids gpi-eGFP and memb-eGFP-mCherry. The medium was replaced by L15 (Invitrogen) supplemented with 10% fetal calf serum prior to observations 24 h after transfection. The eGFP (N)-terminus was tagged with the mouse Thy-1 glycosylphosphatidylinositol (GPI) anchoring sequence, which directs the fusion protein to the outer leaflet of the plasma membrane. The memb-eGFP-mCherry was constructed as previously described (28). The translated protein is eGFP in tandem with mCherry with acyl anchors of Lyn at the N-terminus and is therefore directed to the inner leaflet of the plasma membrane.

FLIM images of both U2OS cells transfected with gpi-eGFP and HEK293 cells transfected with memb-eGFP-mCherry were acquired using the previously described TCSPC technique. Total acquisition time for these 128 × 128 pixels FLIM images was adapted to collect around 30 photons per

pixel (for samples exhibiting monoexponential decays) and 100 photons per pixel (for samples with biexponential decays).

Results

Lifetime determination accuracy depends on the total number of photons and channels, as well as the acquisition time window (14). Because both the total number of channels and time window were fixed experimentally, we focused our study on photon numbers. While it is important to minimize cellular stress caused by long FLIM acquisition times, the correct estimation of all fitting parameters is still a challenge when few photons are collected. We thus developed an original approach called AMDI, based on a statistical inflation of FLIM photon numbers, which could correctly estimate fitting parameters even when small numbers of photons were detected. To validate our approach, we initially tested it on simulated data.

Benefits of AMDI on Simulated Histograms

We simulated temporal decays with fluorescence lifetimes corresponding to eGFP, rhodamine B and rhodamine 6G (2.7, 1.6, and 4 ns, respectively (29)). To determine the reliability of the fitting method in estimating fluorescence lifetimes, we calculated the accuracy defined as

$$\mathrm{Acc} = 1 - \frac{\tau_r - \tau_{\mathrm{me}}}{\tau_r} \qquad (6)$$

With τ_r, the real lifetime value and τ_{me}, the estimated lifetime obtained by fit. Based on statistical laws (30), we considered that an accuracy between 0.9 and 1.1 reflected a robust lifetime estimation.

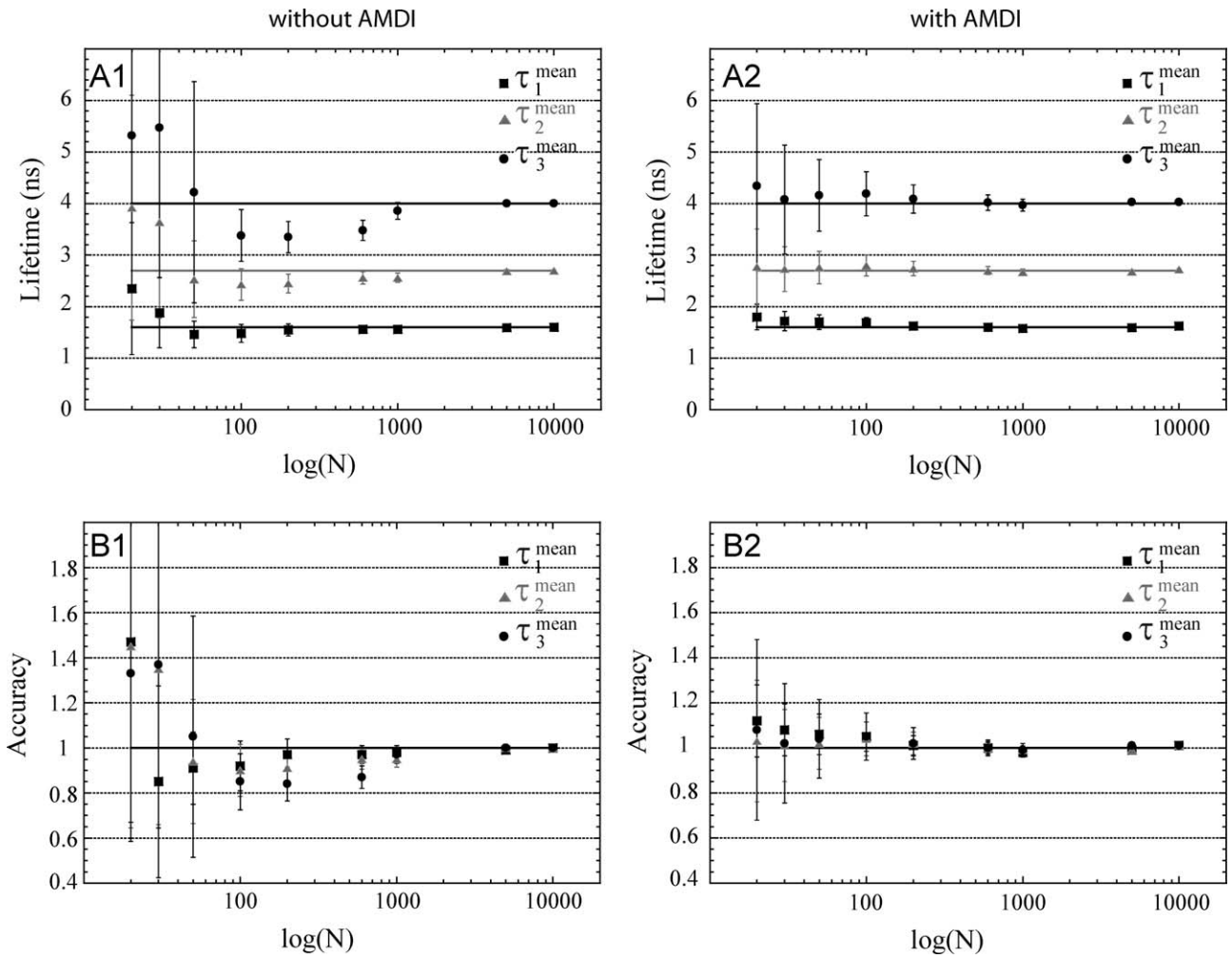

Figure 2. Comparison of lifetime estimations for simulated monoexponential decays with and without AMDI. We represented the fluorescence lifetime estimations as a function of the number of photons *N* with (**A2**) or without (**A1**) AMDI implementation. Three different fluorescence lifetimes—represented by continuous lines—were considered: 1.6, 2.7, and 4 ns (corresponding respectively to rhodamine B, eGFP, and rhodamine 6G). To further demonstrate the superiority of the AMDI approach, we also display the accuracy of lifetime estimation with (**B2**) and without (**B1**) AMDI. In all graphs, markers with error bars represent the mean fluorescence lifetime and standard deviations of 16,384 simulated histograms.

To demonstrate the potential of the AMDI algorithm, we first studied simulated histograms with monoexponential decay. As shown on Figure 2, the accuracy of the standard fitting method is poor when few photons are collected (for instance, $Acc < 0.9$ with 600 photons for long lifetime value), and becomes acceptable ($Acc > 0.95$) when the number of photons is greater than 1,000. We also noted that the correct estimation of fluorescence lifetime depended on how long actual lifetimes were. At least 1,000 photons were required to correctly estimate long lifetimes (4 ns), whereas 600 photons were enough for intermediate lifetimes (2.7 ns) and 50 photons for short lifetimes (1.6 ns).

Significant differences in the accuracy of lifetime estimation were observed when performing the Adaptive Monte Carlo Data Inflation algorithm before the standard fitting method, (Fig. 2). We first noted that, even for photon numbers as low as 20, accuracy was always comprised between 0.9 and 1.1, which represents a 30-fold improvement compared to the standard fitting method. Second, we found that the lowest number of photons needed to correctly estimate short lifetime values (1.6 ns) with AMDI was 30 photons, and 20 photons for medium (2.7 ns) and long lifetimes (4 ns) respectively. In other words, by using the AMDI algorithm, acquisition times may be divided by 50 for long lifetimes, 30 for intermediate lifetimes, and 1.5 for short lifetimes, respectively.

We also tested the efficiency of the AMDI algorithm on simulated histograms with biexponential decays (with $a_1 = 0.3$, $\tau_1 = 1.6$ ns, and $\tau_2 = 4$ ns) and the results are presented in Figure 3. For total photon numbers below 50,000, and without the AMDI algorithm, the standard fitting method overestimated both fluorescence lifetimes, and the corresponding accuracy factor was greater than 1.2. However, mean lifetime ($\tau_m = a_1\tau_1 + (1 - a_1)\tau_2$) was estimated correctly, because the

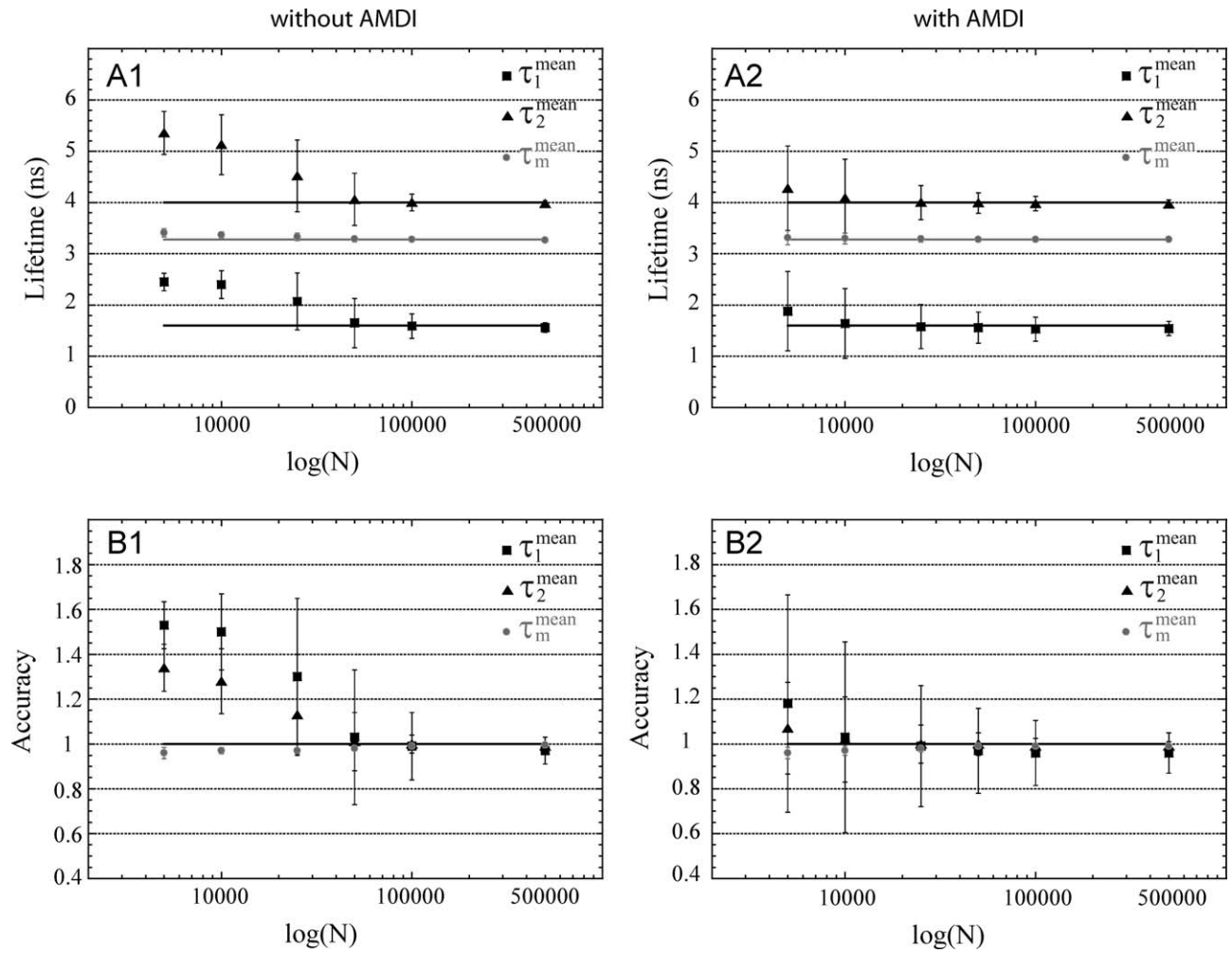

Figure 3. Improvement of lifetime estimations using AMDI for simulated biexponential decays. We performed Monte Carlo simulations to generate 16,384 biexponential intensity decays with parameters: $a_1 = 0.3$, $\tau_1 = 1.6$ ns (lifetime of rhodamine B), and $\tau_2 = 4$ ns (lifetime of rhodamine 6G), which corresponds to a mean lifetime $\tau_m = a_1\tau_1 + (1 - a_1)\tau_2 = 3.28$ ns. The estimations of both fluorescence lifetimes (τ_1 and τ_2) and mean lifetime (τ_m) obtained with and without AMDI are represented respectively in (**A2**) and (**A1**). The corresponding accuracy is also plotted with and without AMDI in (**B2**) and (**B1**). Median fluorescence lifetimes are indicated with markers, and error bars correspond to the interquartile range.

a_1 coefficient was overestimated (data not shown). In other words, the standard fitting method can estimate mean fluorescence lifetime correctly, but requires at least 50,000 photons to estimate all fitting parameters.

With the AMDI algorithm, the number of photons needed for a correct estimation was divided by 10. In fact, 5,000 photons were enough to estimate both fluorescence lifetimes (τ_1 and τ_2) with an accuracy below 1.2. In summary, thanks to the AMDI algorithm, the correct estimation of all fitting parameters is now possible with smaller photon numbers, even if multiple fluorescent species are present.

AMDI Benefits for FLIM Imaging in Living Cells

To demonstrate that the AMDI algorithm could estimate *in vivo* lifetime values correctly, we analyzed FLIM images of live cells transfected with gpi-eGFP. The gpi protein is present in the membrane of U2OS cells (as shown on Fig. 4). To minimize cellular stress, acquisition time was kept short (90 s), compared to the 300 s needed for standard FLIM experiments (300 s). This meant that the mean number of collected photons per pixel was below 30. Without the AMDI algorithm, the standard fitting method was unable to correctly estimate the fluorescence lifetime of the gpi-eGFP, when we applied a binning (which consists in adding the intensity profiles of neighboring pixels included in a square whose surface is $(2n + 1)^2$) of factor $n = 0$ because the number of photons was too small (image not shown). As shown on Figure 4C, the mean lifetime of gpi-eGFP was largely overestimated (around 3.6 ns), compared to $\tau_{mean} = 2.4$ ns using standard FLIM acquisition conditions (300 s and $n = 3$).When the AMDI algorithm was applied, the number of photons per pixel was statistically inflated, and the accuracy of the mean fluorescence lifetime estimation drastically improved ($\tau_{mean} = 2.4$ ns with $n = 0$), although the standard deviation σ was large

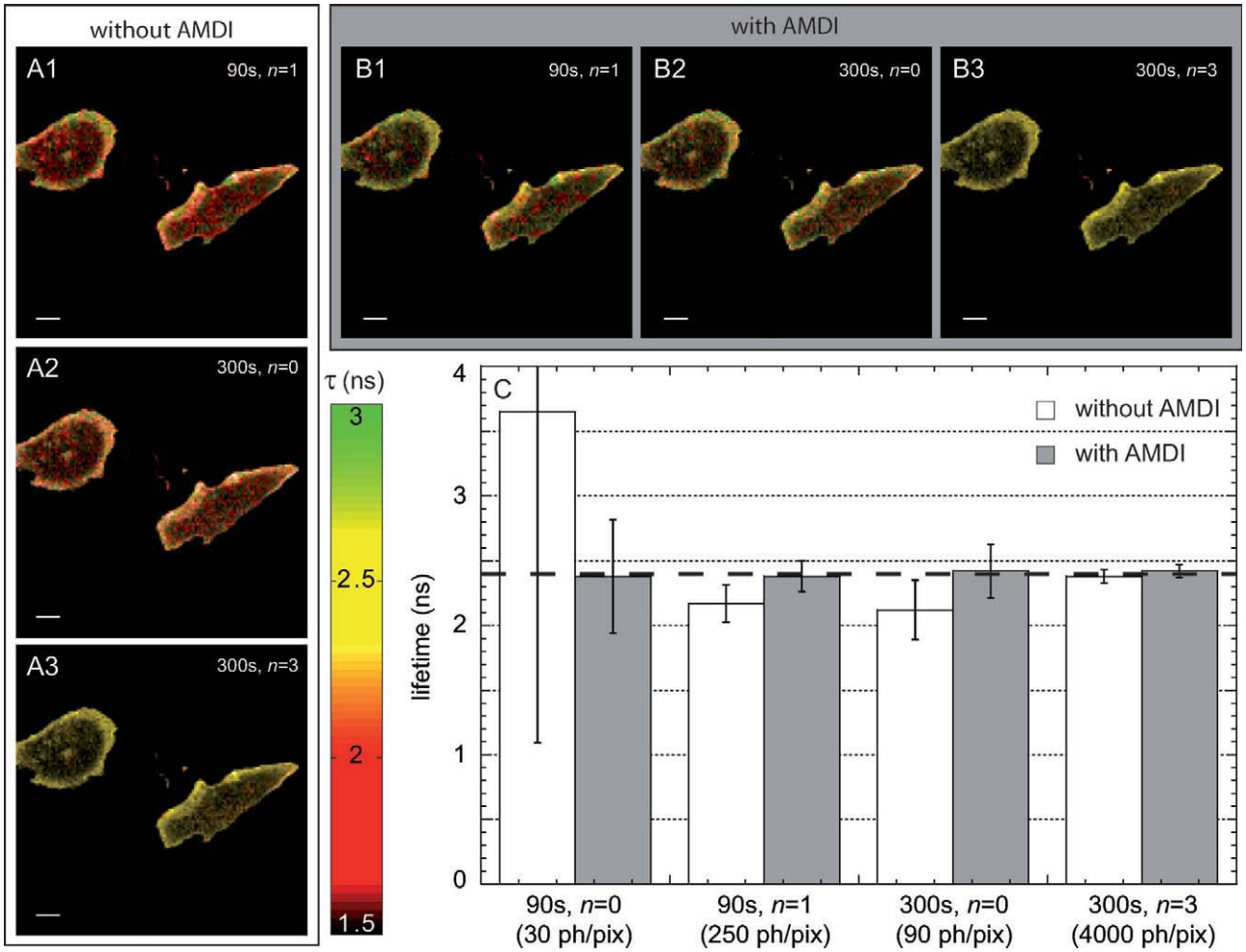

Figure 4. Improvement of fluorescence lifetime measurements using AMDI *in vivo*. FLIM images of U2OS cells transfected with gpi-eGFP are presented after applying (**B**) or not (**A**) the AMDI algorithm. Three distinct conditions were considered: (1) 90 s acquisition time with a spatial binning $n = 1$, (2) 300 s acquisition time with $n = 0$, and (3) 300 s acquisition time with $n = 3$. Scale bar: 10μm. Mean fluorescence lifetimes, standard deviations and mean photon numbers per pixel of each FLIM image are indicated on (**C**). This experiment demonstrates that in contrast to the standard fitting method, the AMDI algorithm enables the correct estimation of gpi-eGFP fluorescence lifetime based on low photon numbers in live cells. [Color figure can be viewed in the online issue which is available at wileyonlinelibrary.com]

(σ = 0.9 ns). It is worth noting that the results obtained in living cell were in excellent agreement with those obtained from *in silico* simulated decays.

To improve both the precision and accuracy of lifetime estimations, photon numbers need to be increased. For this, either the acquisition time or the spatial binning factor n must be increased. Figure 4 shows that the standard fitting method improved but still slightly underestimated the mean fluorescence lifetime (τ_{mean} = 2.17 ns and σ = 0.29 ns) when we applied a binning factor n = 1. The AMDI algorithm allows to estimate mean fluorescence lifetime better (τ_{mean} = 2.38 ns), with a better standard deviation (σ = 0.24 ns). While this spatial binning improved the estimation and the precision of lifetime (with or without AMDI), it is important to note that the spatial resolution of the FLIM image was degraded (Figs. 4A1 and 4B1). In fact, with a spatial binning factor of 1, the lifetime value associated with each pixel corresponds to a surface of 3 × 3 pixels. Consequently, the FLIM image is subjected to an average filtering and some fluorescence lifetime texture is lost. This may cause artifacts and misinterpretations, for example when localizing molecules at the proximity of the plasma membrane.

To avoid this problem and maintain both the best spatial and lifetime resolution possible, we increased acquisition time to 300 s, as is classically used in TCSPC. When using the standard fitting method (without binning factor), the low number of photons (mean around 90 photons per pixel) prevented the correct estimation of fluorescence lifetimes. In agreement with our simulated decay results, the *in vivo* mean lifetime was slightly underestimated (τ_{mean} = 2.12 ns with σ = 0.46 ns). In contrast, when using the AMDI algorithm with n = 0, the gpi-eGFP fluorescence lifetime was correctly estimated (τ_{mean} = 2.40 ns with σ = 0.41 ns) (Fig. 4C). In addition, the image spatial resolution was preserved and corresponds to the initial resolution of the FLIM acquisition system (Fig. 4B2). In other words, the AMDI algorithm correctly estimates fluorescence lifetimes without affecting the spatial resolution of FLIM images, and thus minimizes analysis artifacts due to spatial average filtering.

Having shown that the AMDI algorithm improved fitting estimations of monoexponential decays in living cells, we evaluated its performance in estimating biexponential decays. To this end, we performed FRET experiments on live HEK293 cells expressing eGFP (donor) linked to mCherry (acceptor), fused to a plasma membrane protein. Total acquisition time was 300 s and we initially applied a spatial binning factor of n = 5 to obtain a mean photon number of approximately 7,500 per pixel. As anticipated from our previous results, this number of photons was not sufficient to correctly estimate each fluorescence lifetime with the standard fitting procedure. To address this, we measured in a first FLIM experiment the fluorescence lifetime of the donor alone (2.35 ± 0.13 ns), which corresponds to the τ_2 of FRET experiments (data not shown). We subsequently constrained the second lifetime τ_2 to 2.35 ns, and used the standard fitting method to estimate the first lifetime value τ_1 (data not shown). We found a τ_1 value of 1.16 ± 0.1 ns, which was not in agreement with the value obtained when all parameters are free (τ_1 = 1.38 ± 0.2 ns and τ_2 = 2.8 ± 0.53 ns). We tried increasing the number of photons up to a mean of 20,000 photons per pixel by applying a binning factor of n = 10, but this was still insufficient to estimate both lifetime values correctly, when using the standard fitting method. The measured values of τ_1 = 1.36 ± 0.09 and τ_2 = 2.87 ± 0.2 ns were indeed different from expected values (see Fig. 5C).

In contrast, using the AMDI algorithm, we were able to accurately estimate all fitting parameters, without constraining any parameter, even with mean photon numbers per pixel around 7,500. As indicated in Figure 5C, both fluorescence lifetime values (τ_1 = 1.14 ± 0.58 ns and τ_2 = 2.36 ± 0.62 ns) were in good agreement with expected values, but their interquartile range was wide. We were able to improve the precision of these measurements by applying a spatial binning factor of 10. With n = 10, we obtained: τ_1 = 1.17 ± 0.16 ns and τ_2 = 2.37 ± 0.16 ns.

Note finally that for these numbers of photons, the mean fluorescence lifetime τ_m ($\tau_m = a_1\tau_1 + (1 - a_1)\tau_2$) was always estimated correctly (with or without the AMDI algorithm), and this is consistent with previous Monte Carlo simulations.

Discussion

We here describe an original statistical approach for FLIM combining the well-known statistical technique of bootstrap with an adaptive Parzen kernel. This robust approach statistically inflates initial information, thus significantly reduces the number of photons required to determine all parameters in time domain FLIM experiments. We indeed demonstrated both *in silico* and in living cell that using the AMDI algorithm enables correct lifetime estimation using laser exposure time reduced up to 50 times for fluorescent samples exhibiting monoexponential intensity decays (20 photons per pixel), and 10 times for biexponential decays (corresponding to a minimum of 5,000 photons per pixel), compared to standard fitting method. Thanks to the AMDI algorithm, the precise estimation of all fitting parameters in FRET experiments is now possible even when all parameters are free. Finally, we demonstrated that the AMDI algorithm considerably improves the spatial resolution of FLIM images, by reducing the commonly used spatial binning factor.

While the total number of photons required for a precise lifetime determination using the AMDI algorithm is reduced, the theoretical model developed by Köllner and Wolfrum (14) for describing lifetime precision as a function of the number of photons using the Least Square Method (LSM) remains valid. On the basis of this study, the fluorescence lifetime error $\Delta t/\tau$ of an ideal lifetime determination method ultimately tends towards intensity error $\Delta N/N$ since

$$\frac{\Delta\tau}{\tau} \rightarrow \frac{\sqrt{N}}{N} = \frac{1}{\sqrt{N}} \qquad (7)$$

According to this theoretical limit, for a constant number of photons N, lifetime precision should improve when fluorescence lifetime decreases. This assumption was verified for both

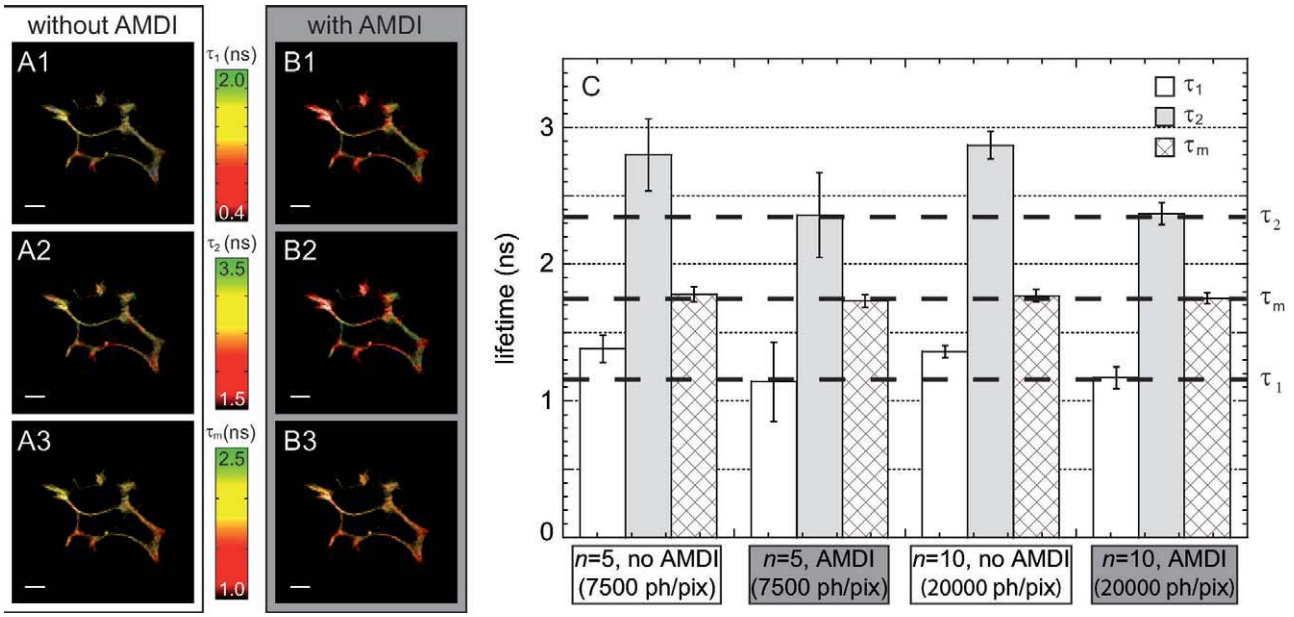

Figure 5. Improvement of FRET measurements *in vivo* using AMDI. FRET experiments were performed on HEK293 living cells expressing the eGFP-mcherry tandem linked to a membrane protein. The fluorescence lifetime images estimated without or with AMDI algorithm are presented respectively in (**A**) and (**B**). For each condition, three FLIM images are shown: (1) first fluorescence lifetime τ_1, (2) second fluorescence lifetime τ_2, and (3) mean lifetime τ_m ($\tau_m = a_1\tau_1 + (1 - a_1)\tau_2$). Scale bar: 10 μm and $n = 5$. For each FLIM image, median fluorescence lifetime values and mean photon per pixel numbers are indicated on (**C**) and error bars correspond to the interquartile range. We also represented expected values for the three fluorescence lifetimes with dashed lines: $\tau_1 = 1.16$ ns, $\tau_2 = 2.35$ ns, and $\tau_m = 1.75$ ns (see text for detail). In contrast to the standard fitting method, the AMDI algorithm makes it possible to accurately estimate all fitting parameters without constraining any of them. [Color figure can be viewed in the online issue which is available at wileyonlinelibrary.com]

our simulated and *in vivo* results. In addition, Eq. (7) suggests that mean fluorescence lifetime determination should be precise even for low photon numbers (N). For example, if 50 photons from a fluorescent sample with a lifetime $\tau = 4$ ns are detected with a FLIM system, the theoretical mean lifetime should be 4 ± 0.6 ns. Of course, values found experimentally differ from these theoretical values. For monoexponential decays, the LSM fitting algorithm does not converge towards the correct mean lifetime when $N < 50$ photons per pixel (this is probably due to the presence of a local rather than global minimum). Performing the AMDI algorithm on the same data computationally inflates the number of photons, and improves the precision of lifetime value estimation using the LSM method. Consequently, the AMDI algorithm is most beneficial to analyze low photon numbers (<100 photons per pixel for monoexponential decays) FLIM images. It is less useful for high photon number images because standard fitting strategies can resolve all fitting parameters equally well. In such cases, the added calculation time required for the AMDI algorithm (a few minutes on a standard computer for a 128×128 pixels FLIM image) becomes superfluous.

To demonstrate the benefits of AMDI in this study, we considered simulated histograms exhibiting both monoexponential and biexponential intensity decays. In this last case, the AMDI algorithm allows reducing the number of photons required to precisely estimate the fluorescence lifetime of each molecular species. Similarly, we demonstrated the benefit of the AMDI algorithm in determining the lifetimes of interacting molecules in FRET experiments. In comparison with standard FLIM image analysis, the AMDI algorithm makes FRET quantification possible with reduced photons numbers (5,000 photons per pixel versus 50,000), and without the need to fix any parameters. In theory, the AMDI algorithm could also improve FLIM image analysis for fluorescent samples emitting more than biexponential intensity decays. In practice, the number of photons required to estimate all fitting parameters (five parameters for triexponential decays) would be so large, that the resulting FLIM image acquisition times would be too long for live cells and tissues.

In addition, we demonstrated the benefit of the AMDI algorithm by fitting simulated and experimental FLIM data with a Levenberg Marquardt algorithm which offers a good compromise between optimization speed and lifetime estimation precision. The benefits of the AMDI algorithm are not limited to this fitting method and may easily be extended to all the minimization algorithms classically used in time domain FLIM image analysis (such as the Newton trust region regression method, which is more robust to dispersive elements). Moreover, it should be noted that since the AMDI algorithm is an inflation of temporal fluorescence intensity decays, it is also compatible with all existing time domain FLIM image analysis strategies (28,31–35).

In this study, we used the AMDI algorithm to reduce the minimum number of photons required for the accurate determination of fitting parameters using the TCSPC technique. This approach may easily be extended to all time domain

FLIM techniques, including multispectral FLIM (or SLIM) experiments. Indeed, the AMDI algorithm should be especially useful for SLIM because, the fluorescence spectral dispersion reduces the number of photons detected compared to standard FLIM. In conclusion, because of its simplicity, robustness and versatility, the AMDI algorithm can be of general use in time domain fluorescence lifetime imaging.

Acknowledgments

We thank Bernard Vandenbunder (IRI) for fruitful discussions and critical comments on the manuscript. We are grateful to Franck Riquet for providing both gpi-eGFP and memb-eGFP-mCherry plasmids. This work benefited from scientific discussions during the thematic school MiFoBio. We are grateful to the imaging platform BICFaL (Biophotonic and Imaging Core Facility of Lille).

Literature Cited

1. Lippincott-Schwartz J, Snapp E, Kenworthy A. Studying protein dynamics in living cells. Nature Rev Mol Cell Biol 2001;2:444–456.
2. Stephens D, Allan V. Light microscopy techniques for live cell imaging. Science 2003;300:82–86.
3. Lakowicsz JR. Principles of Fluorescence Spectroscopy. New York: Plenum Publishers; 1999.
4. van Munster EB, Gadella TW. Fluorescence lifetime imaging microscopy (FLIM). Adv Biochem Eng Biotechnol 2005;95:143–75.
5. Wallrabe H, Periasamy A. Imaging protein molecules using FRET and FLIM microscopy. Curr Opin Biotechnol 2005;16:19–27.
6. Jares-Erijman EA, Jovin TM. FRET imaging. Nat Biotechnol 2003;21:1387–1395.
7. Leray A, Riquet FB, Richard E, Spriet C, Trinel D, Heliot L. Optimized protocol of a frequency domain fluorescence lifetime imaging microscope for FRET measurements. Microsc Res Tech 2009;72:371–379.
8. Booth MJ, Wilson T. Low-cost, frequency-domain, fluorescence lifetime confocal microscopy. J Microsc Oxford 2004;214:36–42.
9. O'Connor DV, Phillips D. Time-Correlated Single Photon Counting. London: Academic Press; 1984.
10. Becker W, Bergmann A, Hink MA, Konig K, Benndorf K, Biskup C. Fluorescence lifetime imaging by time-correlated single-photon counting. Microsc Res Tech 2004;63:58–66.
11. Waharte F, Spriet C, Heliot L. Setup and characterization of a multiphoton FLIM instrument for protein-protein interaction measurements in living cells. Cytometry A 2006;69A:299–306.
12. Buurman EP, Sanders R, Draaijer A, Gerritsen HC, Vanveen JJF, Houpt PM, Levine YK. Fluorescence lifetime imaging using a confocal laser scanning microscope. Scanning 1992;14:155–159.
13. Krishnan RV, Saitoh H, Terada H, Centonze VE, Herman B. Development of a multiphoton fluorescence lifetime imaging microscopy system using a streak camera. Rev Sci Instrum 2003;74:2714–2721.
14. Köllner M, Wolfrum J. How many photons are necessary for fluorescence-lifetime measurements? Chem Phys Lett 1992;200:199–204.
15. König K, Tirlapur U. Cellular and subcellular perturbations during multiphoton microscopy. In: Sons JW, editor. Confocal and Two-Photon Microscopy: Foundations, Applications and Advances; 2002. Chapter 9, pp 191–206.
16. Squirrell JM, Wokosin DL, White JG, Bavister BD. Long-term two-photon fluorescence imaging of mammalian embryos without compromising viability. Nature Biotechnol 1999;17:763–767.
17. Lodish H, Berk A, Zipursky SL, Matsudaira P, Baltimore D, Darnell J. Molecular Cell Biology, 4th ed. New York: W. H. Freeman; 2000.
18. Moon S, Won Y, Kim DY. Analog mean-delay method for high-speed fluorescence lifetime measurement. Opt Express 2009;17:2834–2849.
19. Grant DM, McGinty J, McGhee EJ, Bunney TD, Owen DM, Talbot CB, Zhang W, Kumar S, Munro I, Lanigan PMP, Kennedy GT, Dunsby C, Magee AI, Courtney P, Katan M, Neil MAA, French PMW. High speed optically sectioned fluorescence lifetime imaging permits study of live cell signaling events. Opt Express 2007;15:15656–15673.
20. Li DU, Rae B, Andrews R, Arlt J, Henderson R. Hardware implementation algorithm and error analysis of high-speed fluorescence lifetime sensing systems using center-of-mass method. J Biomed Opt 2010;15:017006.
21. Krauth W. Statistical Mechanics: Algorithms and Computations. Oxford University Press; 2006.
22. Spriet C, Trinel D, Riquet F, Vandenbunder B, Usson Y, Heliot L. Enhanced FRET contrast in lifetime imaging. Cytometry A 2008;73A:745–753.
23. Becker W. Recording the Instrument Response Function of a Multiphoton FLIM System. Application Note: Becker & Hickl GmbH; 2007.
24. Draper NR, Smith H. Applied Regression Analysis. New York: Wiley-Interscience; 1998.
25. Parzen E. Estimation of a probability density-function and mode. Ann Math Stat 1962;33:1065–1076.
26. Efron B. Rietz lecture—Bootstrap methods—Another look at the jackknife. Ann Stat 1979;7:1–26.
27. Efron B, Tibshirani RJ. An Introduction to the Bootstrap. New York: Chapman & Hall/CRC; 1993.
28. Leray A, Spriet C, Trinel D, Heliot L Three-dimensional polar representation for multispectral fluorescence lifetime imaging microscopy. Cytometry A 2009;75A:1007–1014.
29. ISS Company. Lifetime Data Fluorophores. http://www.iss.com/resources/fluorophores.html.
30. Everitt BS. Cambridge Dictionary of Statistics. Cambridge University Press; 2002.
31. Digman MA, Caiolfa VR, Zamai M, Gratton E. The phasor approach to fluorescence lifetime imaging analysis. Biophys J 2008;94:L14–L16.
32. Padilla-Parra S, Auduge N, Coppey-Moisan M, Tramier M. Quantitative FRET analysis by fast acquisition time domain FLIM at high spatial resolution in living cells. Biophys J 2008;95:2976–2988.
33. Barber PR, Ameer-Beg SM, Gilbey J, Carlin LM, Keppler M, Ng TC, Vojnovic B. Multiphoton time-domain fluorescence lifetime imaging microscopy: Practical application to protein–protein interactions using global analysis. J R Soc Interface 2009;6:S93–S105.
34. Verveer PJ, Squire A, Bastiaens PI. Global analysis of fluorescence lifetime imaging microscopy data. Biophys J 2000;78:2127–2137.
35. Leray A, Spriet C, Trinel D, Blossey R, Usson Y, Héliot L. Quantitative comparison of polar approach versus fitting method in time domain FLIM image analysis. Cytometry Part A 2011;79A:149–158.